ROMS simulation of oceanic circulation off the North coast of Papua New Guinea.

Anaïs Fabregas
Aix-Marseille University 2019/2020
Master 1 : Physical and Biogeochemical Oceanography
OPB 205 : Ocean 3D Modeling
May 6, 2019

Key words: New Guinea Coastal Current, New Guinea Coastal Undercurrent, ROMS, numerical modeling, seasonal change.

Abstract: This report presents the results of a 10 years simulation using ROMS numerical model focused on the coastal currents North of Papua New Guinea. ROMS uses the primitive equations of physical oceanography to model ocean circulation. After setting the parameters of the model for the study area, determining the time and spatial steps; the simulation was ran. The data was then analyzed and compared with the literature to identify the regional currents. We found that the westward New Guinea Coastal Current is intense in Southeast season, and non-existent in the Northwest monsoonal season. The New Guinea Coastal Undercurrent is observed all year round, and intensifies during the Southeast season. The model is validated as it is in agreement with the literature.

Mots-clefs : Courant Côtier de Nouvelle-Guinée, Sous-courant côtier de Nouvelle-Guinée, ROMS, Modélisation numérique, changements saisonniers.

Résumé: Ce rapport présente les résultats d’une simulation sur 10 ans à l’aide du modèle ROMS, centré sur les courants côtiers au nord de la Papouasie-Nouvelle-Guinée. ROMS utilise les équations primitives de la physique océanographique pour modéliser la circulation océanique. Après avoir paramétré le modèle, déterminé les pas de temps et d’espace, la simulation fut lancée. Les résultats ont ensuite été analysés et comparés avec la litérature afin d’identifier les courants régionaux. Nous avons observé un courant côtier de Nouvelle-Guinée intense durant la saison de vents du sud-est, et inexistant sous un régime de vent de mousson du nord-ouest. Le sous-courant côtier de Nouvelle-Guinée est observé tout au long de l’année, et s’intensifie durant la saison de vents du sud-est. Le modèle étant en accord avec la litérature, il est donc validé.

I. Introduction

As part of our masters course OPB 205 : Ocean 3D modeling, we ran a 10 years simulation of ocean circulation in our chosen area of study using the Regional Oceanic Modeling System (ROMS).

I.1 Presentation of the study area

The area of interest for this paper is located North of an equatorial island North of Australia, which is split in half with Papua New Guinea (henceforth PNG) to the East, and the Indonesian island of Papua to the West. The study area is bordered by the Philippines on its western border. In this paper, we study the oceanic circulation of this part of the North Pacific Ocean.

I.1.1 Seasonal changes

The study area is strongly affected by seasonal winds and related monsoonal conditions. During Southern hemisphere winter, from June to August, the Intertropical Convergence Zone (ITCZ) shifts northward, so the prevailing winds over PNG in this season are Southeasterly trades. This is known as the Southeast (SE) season. Conversely, during Southern summer, from December to February, the ITCZ moves south, causing a shift in the northeast trade winds at the equator as they become Northwesterly. This is known as the Northwest (NW) monsoon season (Prentice & Hope, 2006, p.2). Refer to **Table 1** for a summary of each season's characteristics and to **Figure 1** for a map of prevailing winds.

Time of year	Southern winter, Jun-Aug	Southern summer, Dec-Feb
Prevailing winds	Southeasterly, SE	Northwesterly, NW
Name of season in this report	SE season	NW season, monsoon

Table 1: Summary of season name, time of year and prevailing winds.

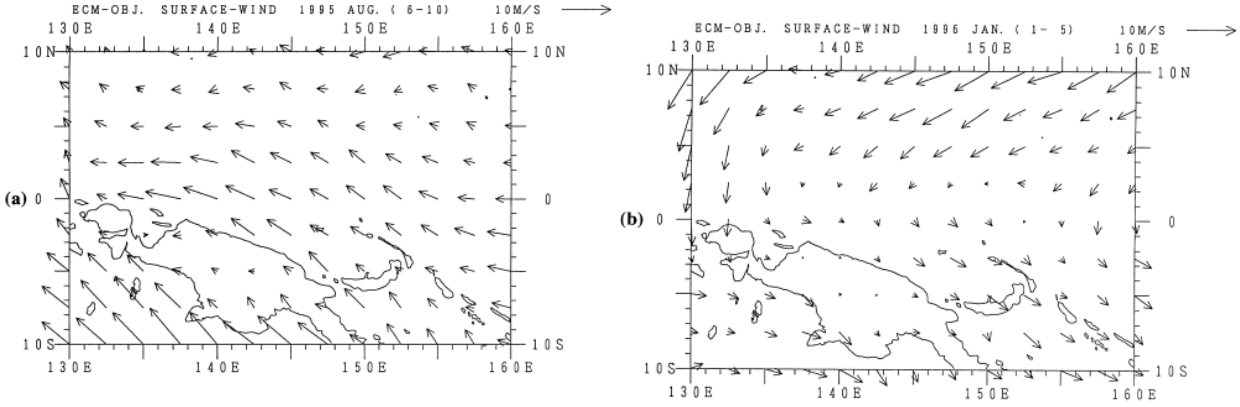

Figure 1: Five day mean surface wind vectors North of PNG (a) August 6–10, 1995; (b) January 1–5, 1996 (Kuroda, 2000, p.109).

I.1.2 Regional ocean currents

As winds affect currents, many of the surface currents in the region vary seasonally with the reversal of winds described above. The South Equatorial Current (SEC) cannot persist against the headwind it faces during the NW season. The Halmaera Eddy (HE) exists from May to October (SE season) and redirects joint water from the SEC and New Guinea Coastal Current (NGCC) into the North Equatorial Counter Current (NECC). The NECC weakens during the NW season as the winds push some of its water to the SE. It is most strongly developed in August (during the SE season). The NGCC flows westward during the SE season which lasts for most of the year (May to November), and reverses under pressure from the NW winds. It thus flows eastward for a short portion of the year (December to March; Wyrtki, 1961, p.23-24).

The New Guinea Coastal Undercurrent (NGCUC) flows at about 220 m deep, and is therefore less affected by the seasonal reversal of winds. Although it persists all year long, it nonetheless weakens during the NW season (Kuroda, 2000, p.103). When it reaches the equator, the NGCUC shifts direction and flows eastward, becoming the Equatorial Undercurrent (EUC; Prentice & Hope, 2006, p.5). Note that this report focuses on the NGCC and NGCUC. Refer to **Figure 2** for a summary of the main currents in the region.

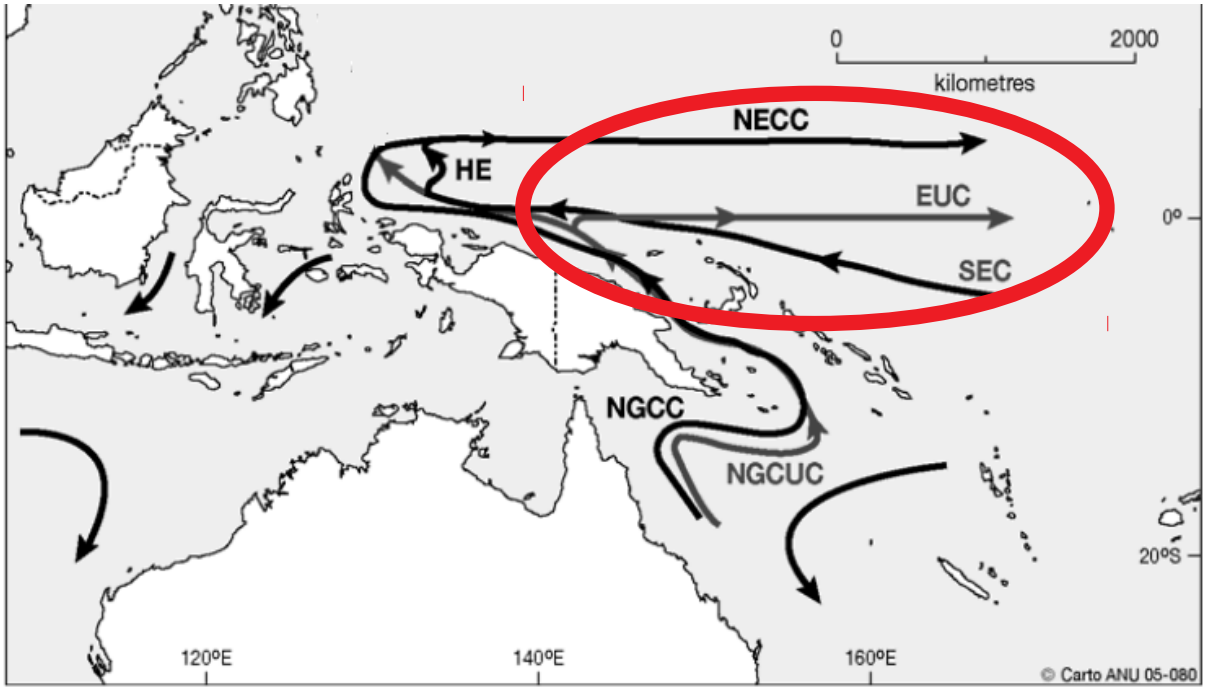

Figure 2: Map of the study area and its main oceanic currents. SEC: South equatorial current, NECC: North equatorial counter current (below 200 m), NGCC: New Guinea Coastal Current, NGCUC: New Guinea Coastal Undercurrent, HE: Halmahera Eddy, EUC: Equatorial Undercurrent. In red was added the approximate location of the WPWP : West Pacific Warm Pool. Map from Prentice & Hope (2006, p.5).

The large amount of islands (Papua, Indonesia, Philippines) in the area acts as a barrier between the Pacific and Indian Ocean. It is also worth noting the presence of the Western Pacific Warm Pool (WPWP) to the North-East of Papua, where some of the warmest surface waters on Earth accumulate after journeying across the Pacific (Refer to Figure 2). The region is characterized by temperatures exceeding 27.5°C at the surface, and salinity values increasing with depth (Prentice & Hope, 2006, p.3).

I.2 Presentation of numerical modeling

Numerical modeling in physical oceanography shares its history with numerical modeling in meteorology. In 1904, Bjerknes phrased the fundamental challenge for making predictions in meteorology: “[...]the necessary and sufficient conditions for a rational solution of the problems of meteorological prediction are the following:
1 :The condition of the atmosphere must be known at a specific time with sufficient accuracy
2: The laws must be known, with sufficient accuracy, which determine the development of one weather condition from another » (Bjerknes, 1904, p.1).

Meteorologists Poincaré and Richardson later identified other prediction challenges such as the non-linearity of the equations governing the state of the atmosphere, as well as the practical issue of numerical calculation that required large resources in an era of limited technology (Doglioli, 2015, p.10).

The advent of the first electronic calculator in 1946 and the exponential increase of computer performances from then on, allowed for more efficient meteorological, then oceanographic predictions. A plethora of ocean models were then developed, giving rise to a number of debates and subsequent improvements to these models (Doglioli, 2015, p.12-13). Among these, the Regional Oceanic Modeling System (ROMS) was developed by Rutgers University and UCLA and is the model used for this study.

II. Methods

II.1 ROMS Primitive Equations

ROMS solves the primitive Navier-Stokes equations of movement for the horizontal (x and y) axes (in Cartesian coordinates) :

$$\frac{\delta u}{\delta t} + \vec{v} . \nabla u - fv = \frac{-1}{\rho} \frac{\delta P}{\delta x} + A_h \nabla_h^2 u + A_v \frac{\delta^2 u}{\delta z^2}$$

$$\frac{\delta v}{\delta t} + \vec{v} . \nabla v + fu = \frac{-1}{\rho} \frac{\delta P}{\delta y} + A_h \nabla_h^2 v + A_v \frac{\delta^2 v}{\delta z^2}$$

Density variations are ignored using the Boussinesq approximation except on the vertical (z) axis where they drive motion. Moreover, vertical buoyancy is balanced by the vertical pressure gradient in the hydrostatic approximation, yielding the following hydrostatic equation for the z axis : $\frac{\delta P}{\delta z}+\rho g=0$

The continuity equation is expressed as follows for an incompressible fluid :

$$\frac{\delta u}{\delta x}+\frac{\delta v}{\delta y}+\frac{\delta w}{\delta z}=0$$

The evolution of salt, temperature, and any other scalar concentration, is given by the advective-diffusive equation :

$$\frac{\delta T}{\delta t}+\vec{v}.\nabla T=K_h\nabla_h^2 T+K_v\frac{\delta^2 T}{\delta z^2}$$

$$\frac{\delta S}{\delta t}+\vec{v}.\nabla S=K_h\nabla_h^2 S+K_v\frac{\delta^2 S}{\delta z^2}$$

Finally, the equation of state is expressed as follows : $\rho=\rho(S,T,P)$

With :

- x, y the horizontal axes ; z the vertical axis
- u, v, w : the x, y, z components of the speed vector $\vec{v}$
- f the Coriolis parameter
- P the pressure ; ρ the density ; g the force of gravity
- T the temperature ; S the salinity
- The indices h and v indicate, respectively, the horizontal axes and the vertical axis
- A is the eddy viscosity coefficient ; K is the eddy diffusivity coefficient. They are present in turbulent flows.

Information for this section comes from WikiROMS (2015), Doglioli (2015), Doglioli & Petrenko (2018).

II.2 ROMS setup

ROMS and associated tools were provided by Croco (2019), from which the following files were downloaded :

- Roms_Agrif_v3.1.1_07_07_2014.tar.gz
- ROMSTOOLS_v3.1.1_07_07_2014.tar.gz
- Utilities_ROMSTOOLS_v3.0_21_12_2012.tar.gz
- COADS05/ COADS05_2006_10_25.tar.gz
- Topo_26_05_2004.tar.gz
- WOA2009 WOA2009_24_06_2011.tar.gz
- GSHHS_coastline_05_02_2013.tar.gz
- ROMS_AGRIF v2.1 & ROMSTOOLS v2.1 User Guide

Our model is set up on an Arakawa C grid, a type of grid designed to be conservative of mass, which is therefore widely used in oceanography (Doglioli, 2019).

II.3 Implementation in the chosen region off PNG

In this course, we used Matlab 2012a software to make our simulation. Parameters had to be changed in a number of scripts to apply ROMS to the study area.

The grid dimensions, resolution, and number of vertical levels were determined to keep the grid to limit grid size to about 10^5 grid cells. The chosen longitude was [121 ; 163]° East, and the chosen latitude [-12 ; 14]° North. Resolution (dl) was 1/3 of a degree, and the number of vertical levels (N) was 32. The following number of grid cells was therefore obtained : $(163-121)*3*(14+12)*3*32=64896$. The relevant changes were made in the matlab script romstools_param.m. Note that the resolution determines the spatial step to be 1/3 of a degree. The spatial step remains constant in degrees, but varies in meters due to map distorsion (see CFL criteria below). The spatial step is also known as the pixel size.

The bathymetry of the region was obtained using the matlab script make_grid.m, see **Appendix A**. Wind stress, Sea Surface Temperature (SST), Sea Surface Salinity (SSS), Surface freshwater flow, surface heat flux, and solar radiation forcings were applied that corresponded with the selected region. These forcings changed every 15 days, depending on the data for this region at this time of year. These forcings were applied using make_forcing.m, and an example of the forcings applied for the wind are provided in **Appendix B**.

Since it is difficult to know the velocity of water entering and exiting the study area, this velocity can be estimated from boundary conditions of Temperature (T) and Salinity (S)

at different times in this region. These boundary conditions were applied using the make_clim.m script, see **Appendix C** for an example of boundary conditions applied. All borders in the study area were considered open, which was written as $obc=[1111]$ in romstools_param.m, corresponding to [South East North West].

The simulation time of 10 years (Y) of 12 months (M) was set in run_roms.csh as :
$set\ NY_{START}=1$; $set\ NY_{END}=10$; $set\ NM_{START}=1$; $set\ NM_{END}=12$.

The Courant-Friedrichs-Lewy (CFL) condition is necessary for the stability of the model. It limits the spatial and time step for to ensure that a water particle cannot travel farther than one grid cell within one time step. The choice of study area determines the spatial step, and the time step remains to be determined using the CFL condition equation below.

$$\Delta t \leq \frac{1}{c} * \left[\frac{1}{\Delta x^2} + \frac{1}{\Delta y^2} \right]^{\left(\frac{-1}{2}\right)}$$

This equation takes into account the fastest speed at which particles can travel, which corresponds to long gravity waves (Doglioli, 2015).

The CFL condition for this model was determined using the matlab script « ad_cfl.m » writen by our Professor Dogioli A. M. (2019) and provided in **Appendix D**. The script takes its input data to calculate the CFL condition from data stored by students in a memo.mat document. This required information is listed in **Table 2** :

Smallest latitudinal cell	Dx min (km)	35.9280
Largest latitudinal cell	Dx max (km)	37.0442
Smallest longitudinal cell	Dy min (km)	36.0031
Largest longitudinal cell	Dy max (km)	37.0441
Number of latitudinal cells	LLm	125
Number of longitudinal cells	MMm	78
Maximum depth	Hmax (m)	5000

Table 2: CFL input data

The external and internal time steps, respectively the NDTFAST and dt[sec] variables, were determined using the ad_cfl.m script, which calculated the time step using the CFL equation explicited above. From this data, we determine the monthly number of iteration (NTIMES), and data saving frequency for instantaneous and averaged output (respectively NWRT and NAVG). These variables must be updated in 3 scripts : roms.in, roms_inter.in, and run_roms.csh. The time steps selected for this simulation are referenced in **Table 3**. Following this setup, the simulation was run.

NDTFAST (sec)	60	External time step
dt[sec] or DTI (sec)	3600	Internal time step of one hour, 24 daily iterations
NTIMES (h)	720	Length of simulation, number of hours in 30 days
NRST (h)	720	Restart file created at the end of each month (roms_rst.nc)
NWRT and NAVG (h)	72	Data saved every 3 days

Table 3: CFL-determined time step for this simulation.

III. Results

Upon reaching the end of the simulation, the script roms_diags.m was used to process the simulation output. The command plot_diags generates a number of plots for averaged diagnostic variables such as kinetic energy, salinity, temperature. An sample plot is provided in **Figure 3** for Temperature, and the plots in their entirety are provided in **Appendix E**.

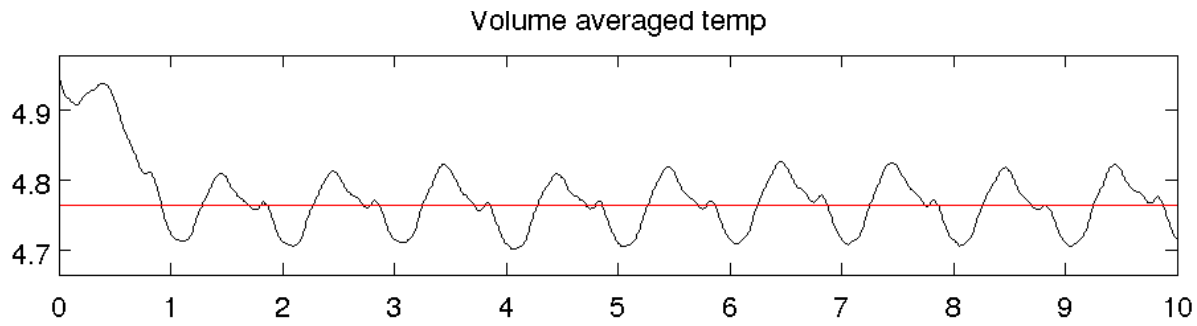

Figure 3: Dignostic plot for the temperature variable. The x axis is time in years.

We later used ROMS' graphical user interface (GUI) using the script roms_gui.m, to visualize the outputs for each month of the simulation. This interface enable us to see the data saved every 3 days fo any given month, and to visualize variables such as surface elevation, temperature, current speed and direction. It also allows us to explore data saved for different depths.

IV. Analysis

Interpreting the diagnostic plots (Appendix E), we can determine the model spin up time until it becomes stable, meaning until we see the same seasonal variation pattern repeating each year around a stable mean. This model is rather stable for all diagnostic variables after the first year of simulation, except for salinity which takes 4 to 5 years to stabilize. Year 8 appears very stable on the diagnostic plots, and we therefore chose to interpret selected results from this year in the following section. We compare our data with the literature that focused on this zone.

IV. 1 Accuracy of the model

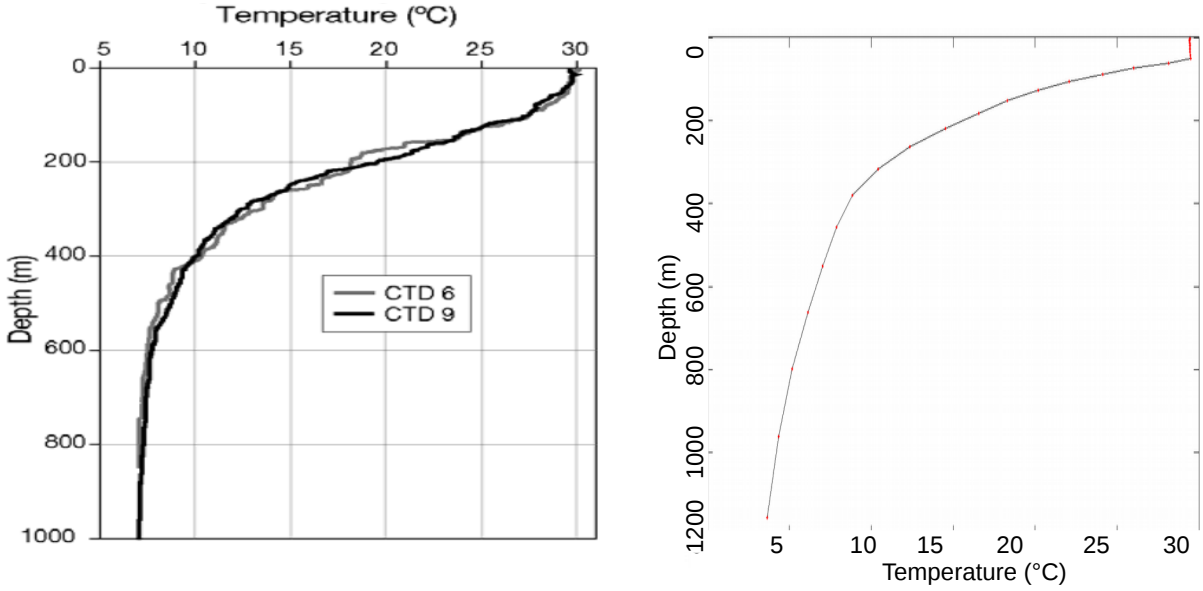

Figure 4: Two vertical temperature profiles made at Cenderawasih Bay in Papua. On the left, CTD graph showing temperature profiles taken by Prentice & Hope (2006, p.4), on the right, vertical profile generated from ROMS data for January of Year 8 of the simulation.

Using ROMS' GUI, we were able to generate vertical temperatures and salinity profiles in areas previously studied in the literature. **Figure 4** shows a CTD temperature profile generated by Prentice & Hope (2006, p.4) in Cenderawasih Bay in Papua, and a vertical temperature profile generated from our model at the same location. These two profiles show similar temperature ranges for similar depths. Similar profiles are provided for salinity in **Appendix F.** These profiles suggest the accuracy of our model in terms of the stability of these variables.

IV.2 New Guinea Coastal Current (NGCC)

Figure 4 is taken during the SE season of Year 8 of the simulation. It shows the presence of the Halmahera Eddy (HE), which redirects surface water from the NGCC into the NECC. We must however note that, due to the eddy's proximity to the open borders of the model, the neighboring islands might be creating some disturbance that could be wrongly identified as the HE. **Figure 5** was taken during the SE season and we can clearly identify the westward-flowing NGCC expected at this period (Prentice & Hope, 2006).

However, our data does not allow us to see the reversal of the NGCC expected during the NW season (Wyrtki, 1961, p.23-24). On **Figure 6**, which is taken in the NW season, we cannot distinguish the NGCC, as there is no noticeable current going in either direction. This is shown by the green along the coast, representing a speed of zero. The headwinds in this season seem strong enough to stop the usual westward flow of the NGCC, but not to create an eastward flow. This could be due to weaker NW wind forcings in our model than in reality.

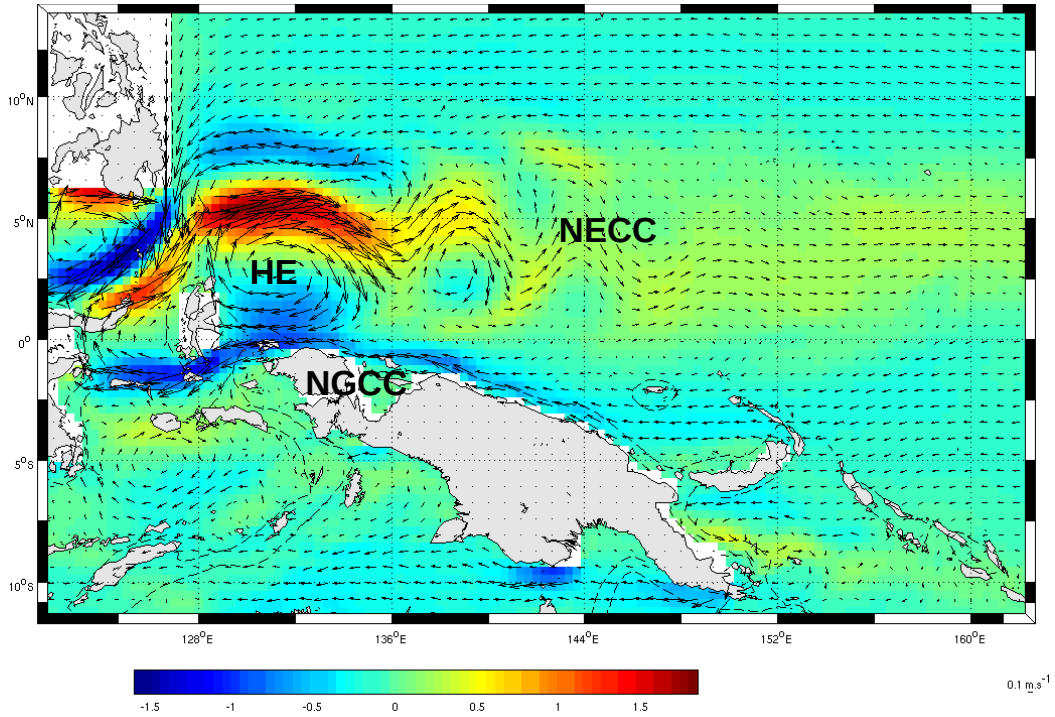

Figure 5 : Image from Year 8, Month 7 (July), at a depth of -10 m. Showing zonal speed, with westward flow in blue and eastward flow in red, in m/s. We notice the presence of the HE, the NGCC, and the NECC. The black arrows are speed vectors.

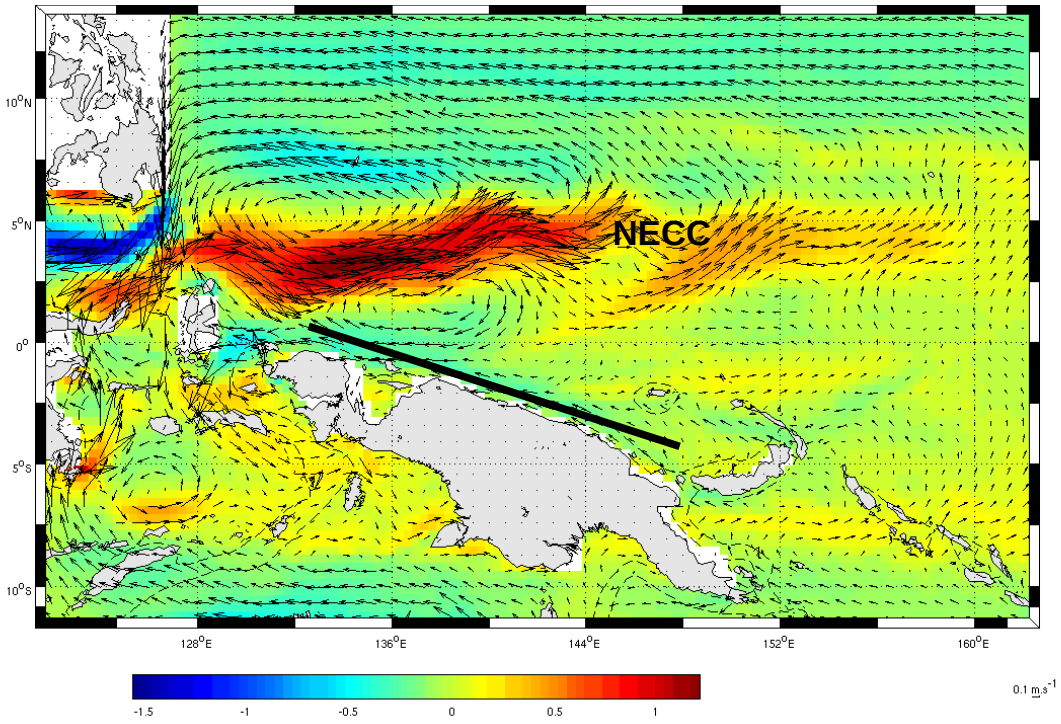

Figure 6 : Image from Year 8, Month 1 (Jan), at a depth of -10 m. Showing zonal speed, with westward flow in blue and eastward flow in red, in m/s. The HE and NGCC have weakened and cannot be distinguished anymore. The black arrows are speed vectors. The black line show the location of the vertical section made to observe the NGCUC, as per the following section.

IV.3 New Guinea Coastal Undercurrent (NGCUC)

In order to see the New Guinea Coastal Undercurrent (NGCUC), we used ROMS' GUI to make vertical sections off the North coast of PNG in order to view the currents present at depth during each season. The section was made at the same location in both seasons (see Figure 6). See Figure 7 for the vertical section profiles in each season.

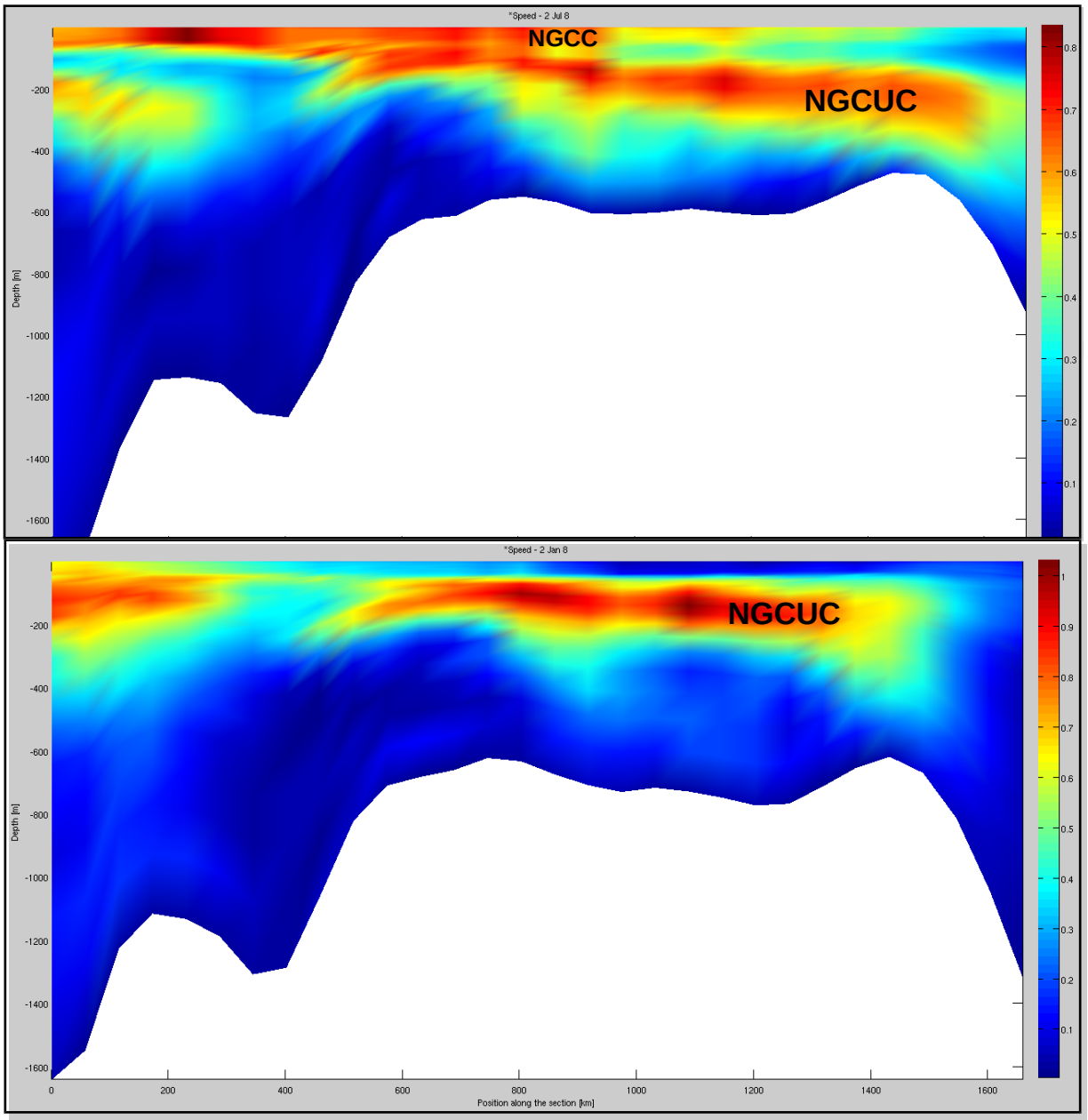

Figure 7: Vertical sections made from West (on the left) to East (on the right) along the North Coast of PNG. The parameter measured is speed in m/s, ranging from 0 in dark blue to 0.8 to 1 m/s in dark red. The x axis shows the position along the section in km, with a section of about 1600 km in total, and the y axis shows depth in m from the surface to -1600. The top graph is for Year 8 Month 7 (July, SE season) and the bottom one is for Year 8 Month 1 (January, NW season).

Figure 7 confirms the previous observations about the NGCC, which is only observed in the SE season, in the thin surface layer between 0 and about 80 m, and its absence in the NW season is clear with the dark blue band representing a null speed at this depth.

Moreover, **Figure 7** shows the presence of the NGCUC, at depths ranging from 150 to 500 m during the SE season (July, top graph) and from 100 to about 350 m during the NW season (January, bottom graph). We find the current's core speed to be located about 200 m deep in January, and slightly deeper in July, around 250 m, which is coherent with the 210-220 m core depth reported in the literature (Kuroda, 2000, p. 107). We can see that the higher limit of the NGCUC is closer to the surface during the NW season (January). No indication of this happening was found in the literature but our hypothesis is that this could be due to the absence of the NGCC in this season, causing the NGCUC to expand in the « free space » above its usual depth.

We also notice that the NGCUC extends deeper during the SE season (July), and as a results the vertical section suggests that this current affects greater areas of water in this season. Although there was no indication of the NGCUC extending deeper in the literature, in situ measurements do observe an intensification of the NGCUC during the SE season (Ueki et al., 2003, p.1), which is coherent with our model. Scientists have found that the NGCUC extends between 150 and 250 m. However, the current profilers used to measure currents did not seem to measure below these depths (Kuroda, 2000, p.107). It would be interesting to have measurements extending further down to 350-400 meters, in order to determine whether our model is correct in continuing to show the presence of the NGCUC at these depths in the SE season (top graph in **Figure 7**).

V. Conclusion

This 10 years simulation was implemented off the coast of PNG in order to observe the coastal currents in this area. We find interesting data showing the seasonal variability of the NGCC and NGCUC, in agreement with the in-situ measurements made in this region. This coherent comparison between our model and the reality, in addition to the stability observed after the first year of the simulation, suggests the accuracy of our model. This analysis would benefit from NGCUC studies at deeper depths, from a possible correction in the model wind forcings, and from perspectives on El Niño which was beyond the scope of this study but does affect this area.

Putting this study in the broader societal context, some companies are planning to launch deep-sea mining operations in the area North of Papua New Guinea. These companies have had to make Environmental Impact Assessments for their project, creating their own studies of deep-sea circulation in the area (Coffey Natural Systems, 2008). Further independent studies from scientists on deep-sea circulation in the area could be useful in determining the impact of such projects.

Bibliography

Bjerknes, V. (1904). The problem of weather prediction, as seen from the standpoints of mechanics and physics. *Meteorologische Zeitschrift*, *18*(6), 663-667. doi: 10.1127/0941-2948/2009/416. Retrieved from: https://pdfs.semanticscholar.org/bfb7/8bf8585f2db51f149412d86df8c7292862da.pdf

Coffey Natural Systems. 2008. Solwara 1 Project Environmental Impact Statement. Retrieved from: http://www.nautilusminerals.com/irm/content/pdf/environment-reports/Appendices%201-3.pdf

Croco. (2019). Croco – Coastal and Regional Ocean COmmunity model. Retrieved from: https://www.croco-ocean.org

Doglioli A. M. (2015). *Notes de Cours et Travaux Dirigés de Modélisation de la Circulation Océanique*, Université d'Aix-Marseille, Marseille, France. Retrieved from: https://people.mio.osupytheas.fr/~doglioli/Doglioli_NotesCoursTD_Modelisation3DOceanique.pdf

Doglioli A. M. & Petrenko A. (2018). *Notes de Cours et Travaux Dirigés de Dynamique des Océans*, Université d'Aix-Marseille, Marseille, France. Retrieved from: https://people.mio.osupytheas.fr/~doglioli/DoglioliPetrenko_NotesCoursTD_DynamiqueOceans.pdf

Doglioli, A. M. (2019). *Présentation des grilles Arakawa* [Lecture Notes]. Université d'Aix-Marseille, Marseille, France

Kuroda, Y. (2000). Variability of Currents off the Northern Coast of New Guinea. *Journal of Oceanography*, 56(1), pp.103-116.

Prentice, M. L. & Hope, G. (2006). Climate of Papua. Retrieved from: https://www.researchgate.net/publication/230892232_Climate_of_Papua

Ueki, I., Kashino, Y., & Kuroda, Y. (2003). Observation of current variations off the New Guinea coast including the 1997–1998 El Niño period and their relationship with Sverdrup transport. *Journal Of Geophysical Research*, *108*(C7). doi: 10.1029/2002jc001611

WikiROMS. (2015). Equations of Motion - WikiROMS. Retrieved from : https://www.myroms.org/wiki/Equations_of_Motion

Wyrtki, K. (1961). *Physical oceanography of the Southeast Asian waters*. La Jolla, Calif.: University of California, Scripps Institution of Oceanography. pp.22-24. Retrieved from : https://escholarship.org/uc/item/49n9x3t4

Appendices

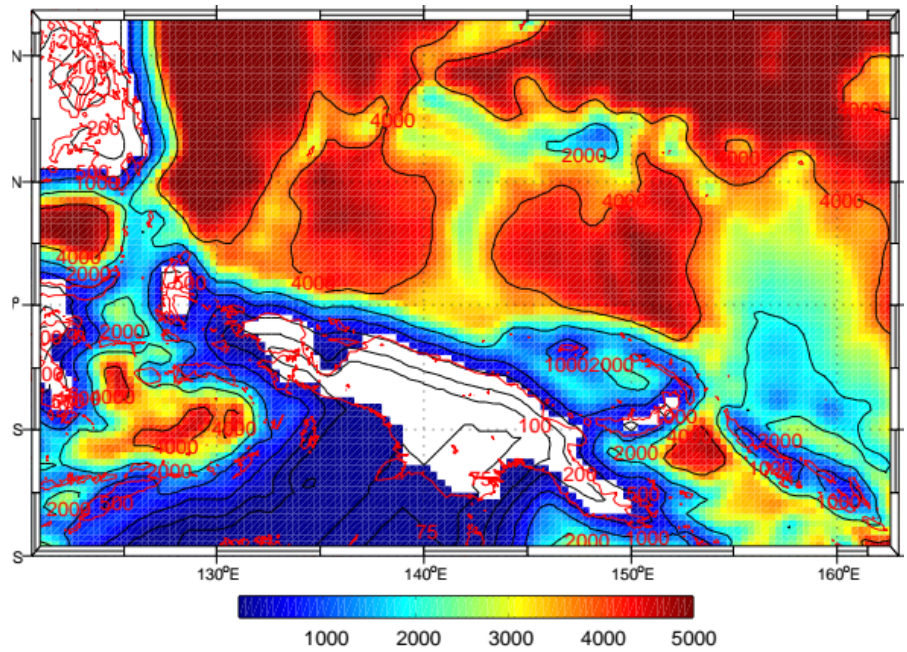

Appendix A : Bathymetry of the region using make_grid.m. Depth in legend is in meters.

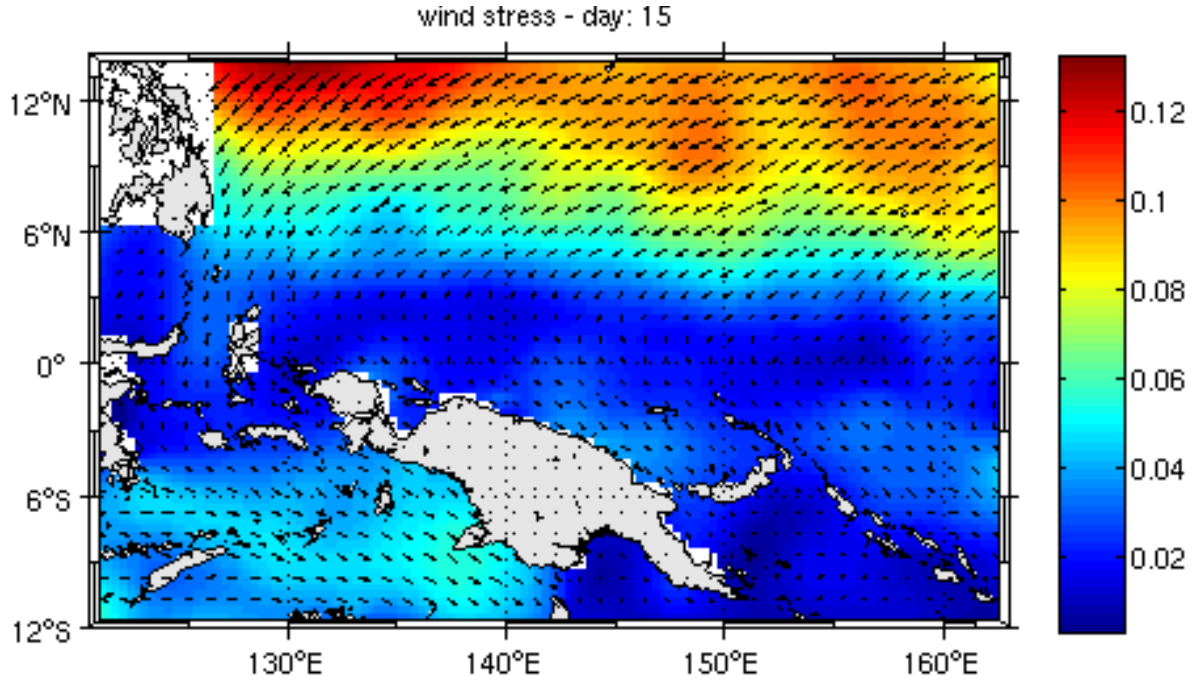

Appendix B : Example of forcings applied using make_forcing for the wind on January 15th of each simulation year. Wind speed in legend is in m/s.

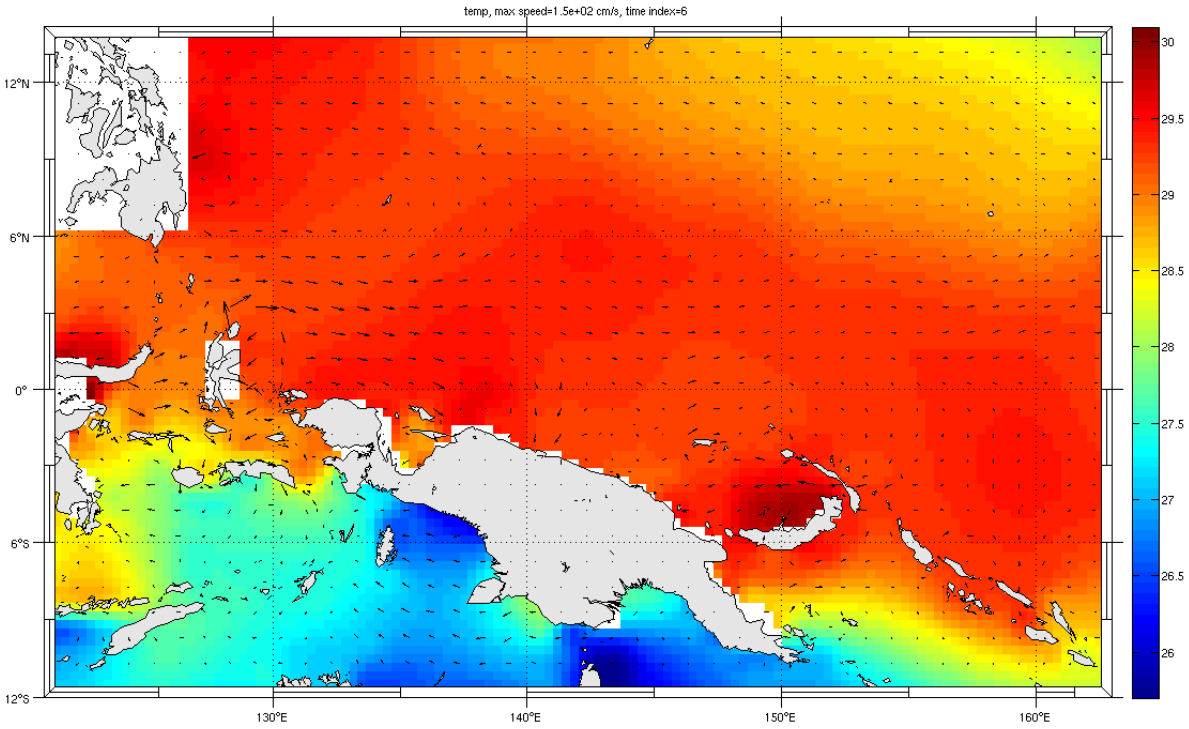

Apppendix C : Example of figure for the temperature boundary condition applied in June, obtained using make_clim.m. Temperature in legend is in °C.

Appendix D : Matlab script ad_cfl.m used to determine the CFL condition for the study area. The script was developed by our Professor Doglioli Andrea M. (2019).

```
clear;close all;

%%% Andrea
% This script compute the internal timestep
% on the basis of ourant-Friedrichs-Levy criterion
% and provide time parameter values for you run
%%%%%%%%%%%%%%%%%%%%%%%%%%%%%%%%%%%%%%%%%%%%%%%%%%%%%%%%%%%%%%%%
load memo
disp([' LLm = ',num2str(LLm)])
disp([' MMm = ',num2str(MMm)])
disp([' Min dx=',num2str(dxmin),' km - Max dx=',num2str(dxmax),' km'])
disp([' Min dy=',num2str(dymin),' km - Max dy=',num2str(dymax),' km'])
%
% Read in the grid
%
nc=netcdf(grdname);
Lp=length(nc('xi_rho'));
Mp=length(nc('eta_rho'));
hmax=max(max(nc{'h'}(:)));
result=close(nc);
disp([' Hmax=',num2str(hmax),' m'])
%%%%%%%%%%%%%%%%%%%%%%%%%%%%%%%%%%%%%%%%%%%%%%%%%%%%%%%%%%%%%%%%

disp(' ');
Hmax=input(' Hmax [m] ? ');
Dx=  input(' Dx [km]  ? ');
Dy=  input(' Dy [km]  ? ');

disp(' ');
DTEcfl=1/(2*sqrt(9.8*Hmax))*1/sqrt(1/(Dx*1000)^2+1/(Dy*1000)^2);
       disp([' DTEcfl  = ',num2str(DTEcfl),' [sec]']);

NTDFAST=input(' NTDFAST ? ');

DTI=NTDFAST*DTEcfl;
       disp([' DTI     = ',num2str(DTI),' [sec]']);

CHECK=rem(86400,DTI);
while CHECK~=0
 disp(' ');
 disp([' !!!Warning!!! 86400/DTI is not an integer']);
 disp(' ');
    DTE=input(' your DTE ? ');
 NTDFAST=input(' NTDFAST  ? ');
 DTI=NTDFAST*DTE;
       disp([' DTI      = ',num2str(DTI),' [sec]']);
 CHECK=rem(86400,DTI);
end

DAYcoeff=86400/DTI;
MONTH=30*DAYcoeff;
disp(' ');
disp(' OK!, summarizing: ');
disp('---------------------------- ');
disp(' NTIMES   dt[sec]  NTDFAST')
disp([' ',num2str(MONTH),'    ',num2str(DTI),'    ',num2str(NTDFAST)])
disp('---------------------------- ');
disp([' 1 Day  = ',num2str(DAYcoeff),' iterations']);
disp([' 2 Days = ',num2str(2*DAYcoeff),' iterations']);
disp([' 5 Days = ',num2str(5*DAYcoeff),' iterations']);
disp('---------------------------- ');
```

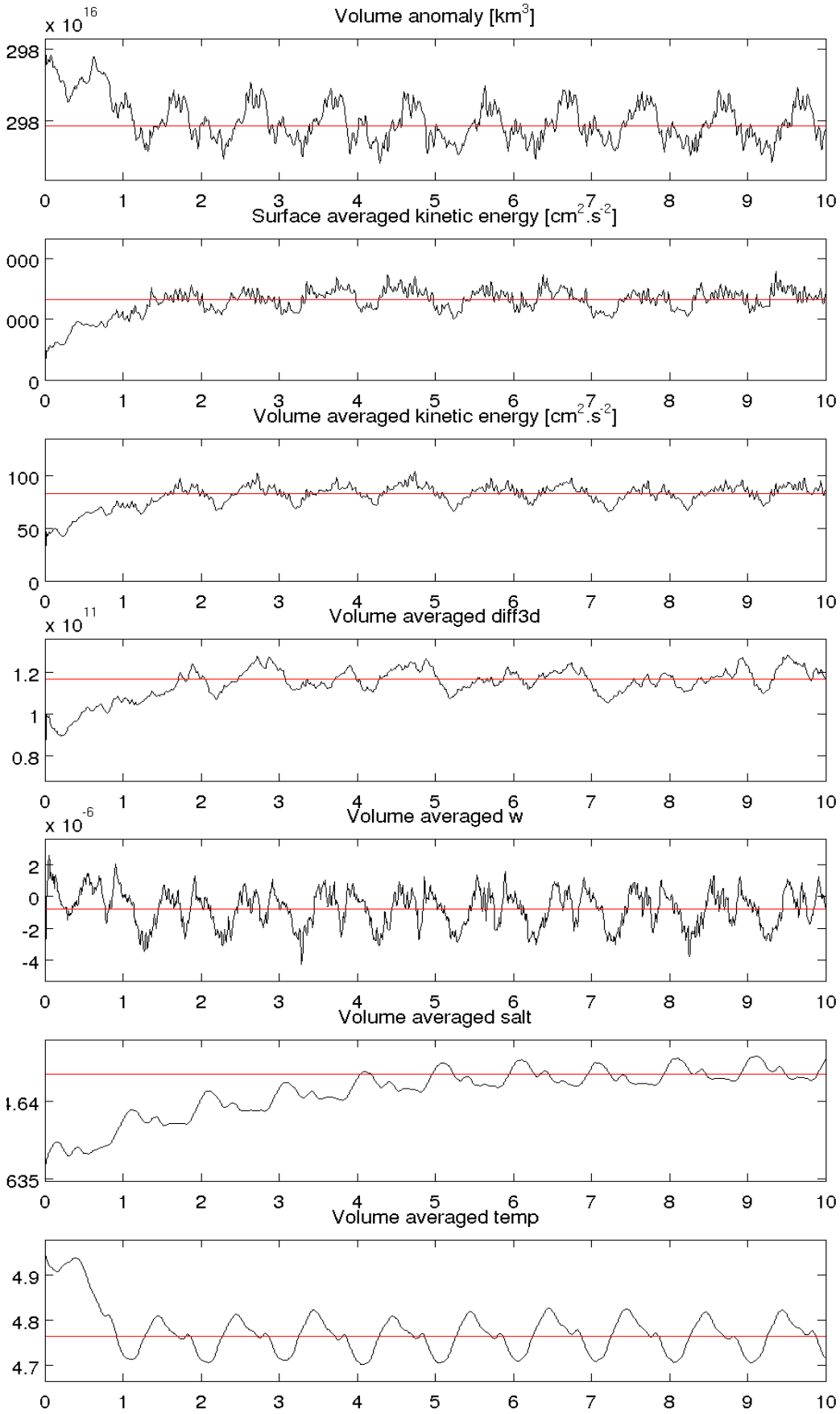

Appendix E : Diagnostic averaged variables of the simulation, generated using roms_diags.m and plot_diags. The x axis is time in years.

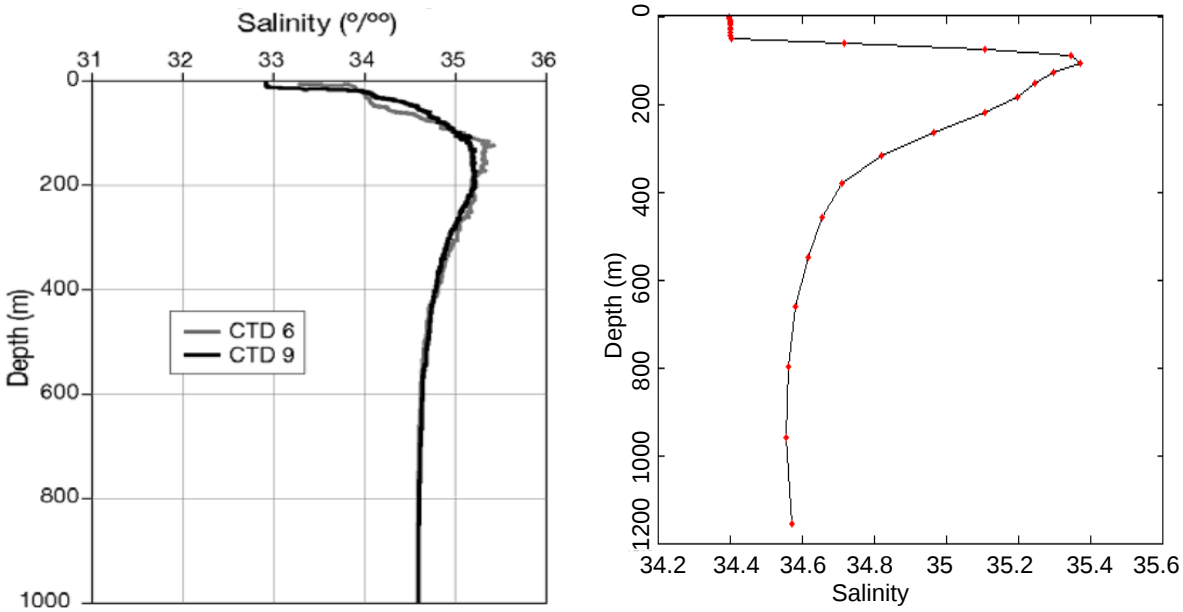

Appendix F: Two vertical salinity profiles made at Cenderawasih Bay, Papua. On the left, CTD graph showing salinity profiles taken by Prentice & Hope (2000, p.4); on the right, vertical profile generated from ROMS data for January of Year 8 of the simulation.